

Swift Observations of GRB 140419A

F.E. Marshall (NASA/GSFC), A. Maselli (INAF-IASFPA) and N.P.M. Kuin (MSSL-UCL) for the Swift team

1. Introduction

At 04:06:51 UT, the Swift Burst Alert Telescope (BAT) triggered and located GRB 140419A (trigger=596426) (Marshall *et al.* GCN Circ. [16118](#)). Swift slewed immediately to the burst. At the time of the trigger, the initial BAT position was 89° from the Sun (6.7 hours East) and 131° from the 83%-illuminated Moon. **Table 1** contains the best reported positions from Swift, and the latest XRT position can be viewed at http://www.swift.ac.uk/xrt_positions.

Marshall *et al.* (GCN Circ. [16118](#)) reported the discovery with UVOT of an optical afterglow. Zheng *et al.* (GCN Circ. [16119](#)) reported the position from KAIT for the optical afterglow of this GRB. Tanvir *et al.* (GCN Circ. [16125](#)) determined a redshift of 3.956 from Gemini. **Table 2** is a summary of GCN Circulars about this GRB from observatories other than Swift.

Standard analysis products for this burst are available at http://gcn.gsfc.nasa.gov/swift_gnd_ana.html.

2. BAT Observations and Analysis

As reported by Baumgartner *et al.* (GCN Circ. [16127](#)), the BAT ground-calculated position is RA, Dec = 127.001, 46.234 deg, which is RA (J2000) = 08^h28^m00.4^s Dec (J2000) = +46°14'03.7" with an uncertainty of 1.0 arcmin, (radius, sys+stat, 90% containment). The partial coding was 33%.

The mask-weighted light curve (**Figure 1**) shows two slightly overlapping clusters of peaks, starting at $\sim T-10$ s, peaking at $\sim T+10$ and $\sim T+51$ s, and ending at $\sim T+220$ s. T_{90} (15-350 keV) is 94.7 ± 11.0 s (estimated error including systematics).

The time-averaged spectrum from T-8.69 to T+222.32 s is best fit by a simple power-law model. The power law index of the time-averaged spectrum is 1.21 ± 0.04 . The fluence in the 15-150 keV band is $1.59 \pm 0.03 \times 10^{-5}$ erg cm⁻². This fluence is larger than that of 96% of the long GRBs in the Second BAT GRB Catalog (Sakamoto *et al.* 2011). The 1-s peak photon flux measured from T+51.42 s in the 15-150 keV band is 4.9 ± 0.2 ph cm⁻² s⁻¹. All the quoted errors are at the 90% confidence level.

The results of the batgrbproduct analysis are available at http://gcn.gsfc.nasa.gov/notices_s/596426/BA/.

3. XRT Observations and Analysis

Maselli *et al.* (GCN Circ. [16128](#)) reported the analysis of the initial XRT data. We have analyzed 92 ks of XRT data for GRB 140419A, from 79.9 s to 1297.8 ks after the BAT trigger. The data comprise 1.4 ks in Windowed Timing (WT) mode (the first 5 s were taken while Swift was slewing) with the remainder in Photon Counting (PC) mode. The enhanced XRT position for this burst was given by Osborne *et al.* (GCN Circ. [16124](#)).

The late-time light curve (**Figure 2**) (from T+5.4 ks) can be modeled with a series of power-law decays. The initial decay index is $\alpha=1.58$ (+0.21, -0.16). At T+12.0 ks the decay flattens to an α of 0.96 (+0.14, -0.49) before breaking again at T+28.6 ks to a final decay with index $\alpha=1.55 \pm 0.07$.

A spectrum formed from the WT mode data can be fitted with an absorbed power-law with a photon spectral index of 1.798 (+0.029, -0.017). The PC mode spectrum has a photon index of 1.890 (+0.056, -0.054) and a best-fitting absorption column of 1.42 (+0.59, -0.56) $\times 10^{22}$ cm⁻² at a redshift of 3.956, in addition to the Galactic value of 3.9 $\times 10^{20}$ cm⁻² (Willingale *et al.* 2013). The counts to observed (unabsorbed) 0.3-10 keV flux conversion factor deduced from this spectrum is 3.5 $\times 10^{-11}$ (4.0 $\times 10^{-11}$) erg cm⁻² count⁻¹.

A summary of the PC-mode spectrum is thus:

Galactic foreground: 3.9 $\times 10^{20}$ cm⁻²

Intrinsic column: 1.42 (+0.59, -0.56) $\times 10^{22}$ cm⁻² at z=3.956

Photon index: 1.890 (+0.056, -0.054)

The results of the XRT team automatic analysis are available at http://www.swift.ac.uk/xrt_products/00596426.

4. UVOT Observations and Analysis

The Swift/UVOT began settled observations of the field of GRB 140419A 97 s after the BAT trigger (Kuin and Marshall GCN Circ. [16130](#)). A source consistent with the XRT position is detected in the initial UVOT exposures. **Table 3** gives preliminary magnitudes using the UVOT photometric system (Breeveld *et al.* 2011, AIP Conf. Proc., 1358, 373). No correction has been made for the expected extinction in the

Milky Way corresponding to a reddening of E_{B-V} of 0.03 mag. in the direction of the GRB (Schlegel *et al.* 1998).

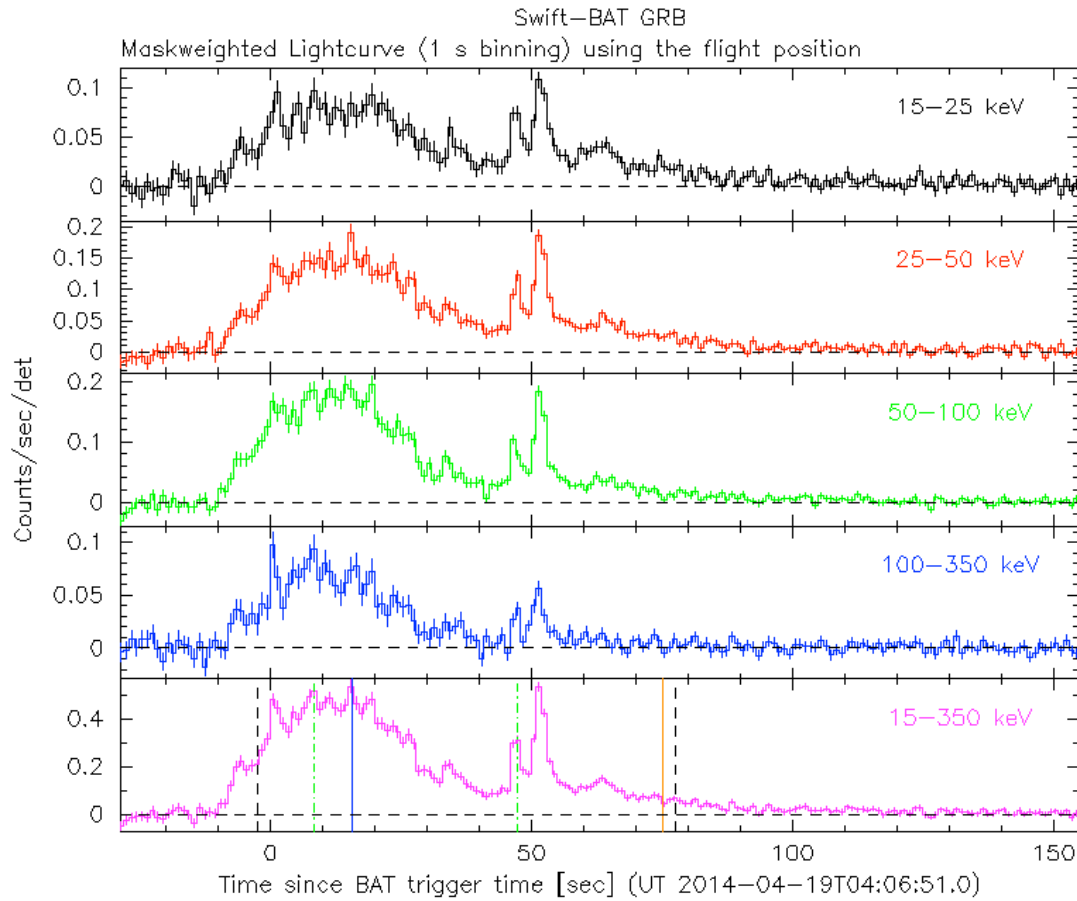


Figure 1. The BAT mask-weighted light curve in the four individual and total energy bands. The units are counts s^{-1} illuminated-detector $^{-1}$.

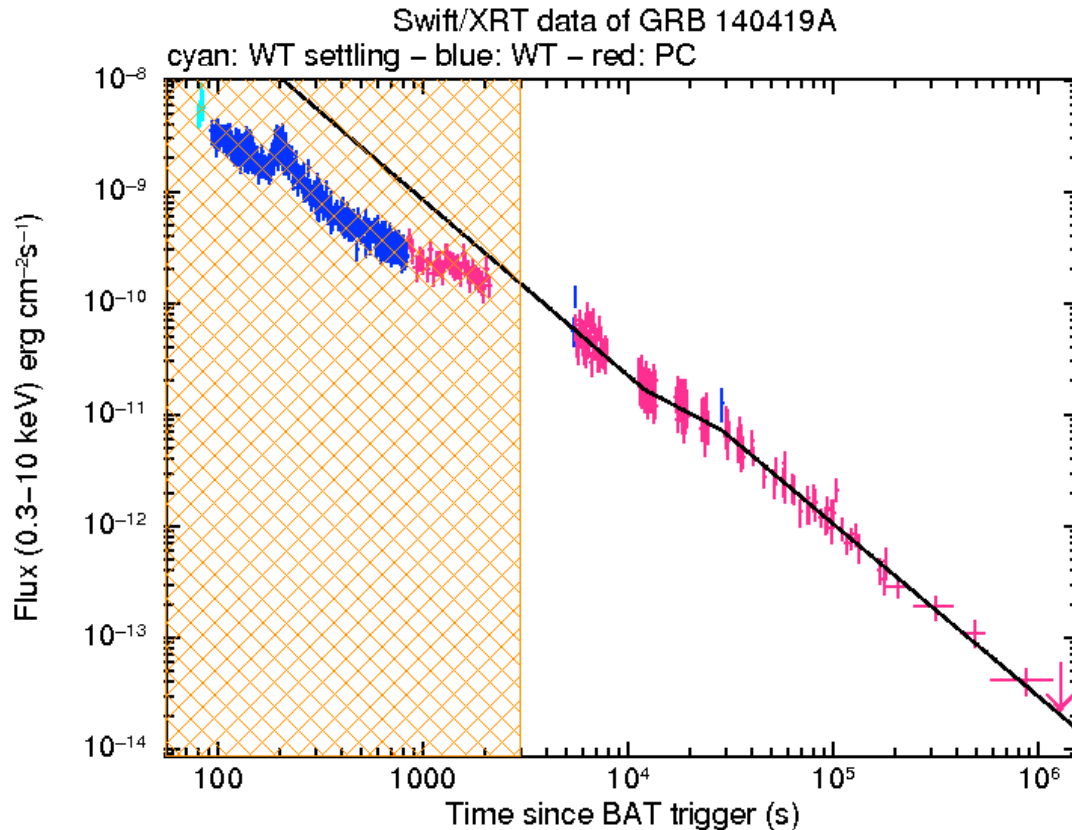


Figure 2. The XRT light curve. Data from the crosshatched region are not included in the fit.

RA (J2000)	Dec (J2000)	Error	Note	Reference
08 ^h 27 ^m 57.56 ^s	+46°14'25.3"	0.50"	UVOT-refined	Kuin and Marshall GCN Circ. 16130
08 ^h 27 ^m 57.51 ^s	+46°14'24.1"	1.4"	XRT-final	UKSSDC
08 ^h 27 ^m 57.53 ^s	+46°14'24.3"	1.5"	XRT-enhanced	Osborne <i>et al.</i> GCN Circ. 16124
08 ^h 28 ^m 00.4 ^s	+46°14'03.7"	1.0'	BAT-refined	Baumgartner <i>et al.</i> GCN Circ. 16127

Table 1. Positions from the Swift instruments.

GCN Report 468.1 07-May-14

Band	Authors	GCN Circ.	Subject	Observatory	Notes
Optical	Zheng <i>et al.</i>	16119	KAIT optical candidate	KAIT	detection
Optical	Guver <i>et al.</i>	16120	ROTSE-III Detection of Optical Counterpart	ROTSE	detection
Optical	Butler <i>et al.</i>	16121	RATIR Optical and NIR Observations	RATIR	detection
Optical	Tanvir <i>et al.</i>	16125	Gemini-N redshift	Gemini	redshift
Optical	Hentunen <i>et al.</i>	16126	T24 optical observations	iTelescope	detection
Optical	Cenko and Perley	16129	P60 Observations	Palomar 60- inch	detection
Optical	Kuroda <i>et al.</i>	16131	MITSuME Okayama Optical Observation	MITSuME Okayama	detection
Optical	Kuroda <i>et al.</i>	16132	MITSuME Ishigakijima Optical Observation	MITSuME Ishigakijima	detection
Optical	Pandey and Kumar	16133	Optical Observations	Nainital	detection
Optical	Littlejohns <i>et al.</i>	16136	Continued RATIR Optical and NIR Observations	RATIR	detection
Optical	Zheng <i>et al.</i>	16137	KAIT Refined Analysis	KAIT	detection
Optical	Xu <i>et al.</i>	16138	NOT optical observations	NOT	
Optical	Littlejohns <i>et al.</i>	16139	Continued RATIR Optical and NIR Observations	RATIR	detection
Optical	Xu	16140	Refined NOT photometry	NOT	

GCN Report 468.1 07-May-14

Optical	Volnova <i>et al.</i>	16141	Mondy optical observations	Mondy	detection
Optical	Choi <i>et al.</i>	16149	LOAO R-band observations	LOAO	
Optical	Volnova <i>et al.</i>	16168	Continued Mondy optical observations	Mondy	detection
Radio	Perley	16122	CARMA early 3mm detection	CARMA	detection
Gamma-ray	Golenetskii <i>et al.</i>	16134	Konus-Wind observation	Konus-Wind	$E_{\text{peak}}=293 \pm 84 \text{ keV}$ Fluence= $5.8 (-1.9,+2.8) \times 10^{-5} \text{ erg cm}^{-2}$

Table 2. Summary of GCN Circulars from other observatories sorted by band and then circular number.

Filter	T _{start} (s)	T _{stop} (s)	Exp(s)	Mag
white	97	246	147	16.2 ± 0.2
v	638	658	19	16.1 ± 0.2
b	564	756	39	18.4 ± 0.2
u	309	2003	362	>21.0
w1	687	707	19	>18.1

Table 3. UVOT observations reported by Kuin and Marshall (GCN Circ. [16130](#)). The start and stop times of the exposures are given in seconds since the BAT trigger. The preliminary detections and 3- σ upper limits are given. No correction has been made for extinction in the Milky Way.

May 5, 2014